Chapter 4 — The Kambalda Nickel Camp

ML Fiorentini

Centre for Exploration Targeting, School of Earth and Environment, The University of Western Australia

Introduction

Nickel sulphide mineralisation was first discovered in the Kambalda Dome in 1966, approximately 70 years after gold was identified. The Kambalda Dome is a doubly plunging anticline cored by granitic intrusions post-dating nickel sulphide mineralisation. Nickel sulphide mineralisation is primarily hosted within the volcanic stratigraphy exposed along the flanks of the intrusions, and occurs as discontinuous to semi-continuous lenticular bodies of mineralisation termed 'ore shoots' (Gresham and Loftus-Hills, 1981).

The Kambalda Dome is hosted within the Kambalda Domain of the Kalgoorlie Terrane, which represents one of the fault-bounded tectonostratigraphic units into which the Eastern Goldfields Superterrane is subdivided (Swager et al., 2002, 2007; Cassidy et al. 2006; Kositcin et al., 2008; Figs 1, 41).

The three main lithostratigraphic sequences of the Kalgoorlie Terrane are: 1) the Kambalda Sequence, 2) the Kalgoorlie Sequence and 3) the Kurrawang and Merougil Sequences (Krapež et al., 2000). Figure 42 schematically illustrates the volcano-sedimentary sequence preserved in the Kambalda and Kalgoorlie Sequences at Kambalda: nickel sulfide mineralisation is mostly localised at the contact between the Lunnon Basalt and Silver Lake Member of the Kambalda Komatiite Formation.

The Kambalda Sequence comprises the Lunnon Basalt, Kambalda Komatiite (Silver Lake Member and Tripod Hill Member), Devon Consols Basalt, Kapai Slate, and Paringa Basalt. The eruption age of the Kambalda Komatiite in the Kambalda Sequence is constrained by contemporaneous komatiite and dacite volcanic activity in the Boorara Domain (Trofimovs et al., 2004) and in the Agnew–Wiluna greenstone belt (Fiorentini et al., 2005). Zircon U–Pb age determinations from the dacite volcanic rocks contain an average age of 2707 ± 4 Ma (Kositcin et al., 2008; Claoue-Long et al., 1988; Nelson, 1995, 1997, 1998). Direct Re–Os isotopic age determinations on nickel sulphide mineralisation from Mount Keith generated a comparable isochron age of 2706 ± 36 Ma (Foster et al., 1996). A detrital zircon age of 2692 ± 4 Ma was obtained from the Kapai Slate, which represents an upper age limit for the Paringa Basalt of the Kambalda Sequence (Claoue-Long et al., 1988).

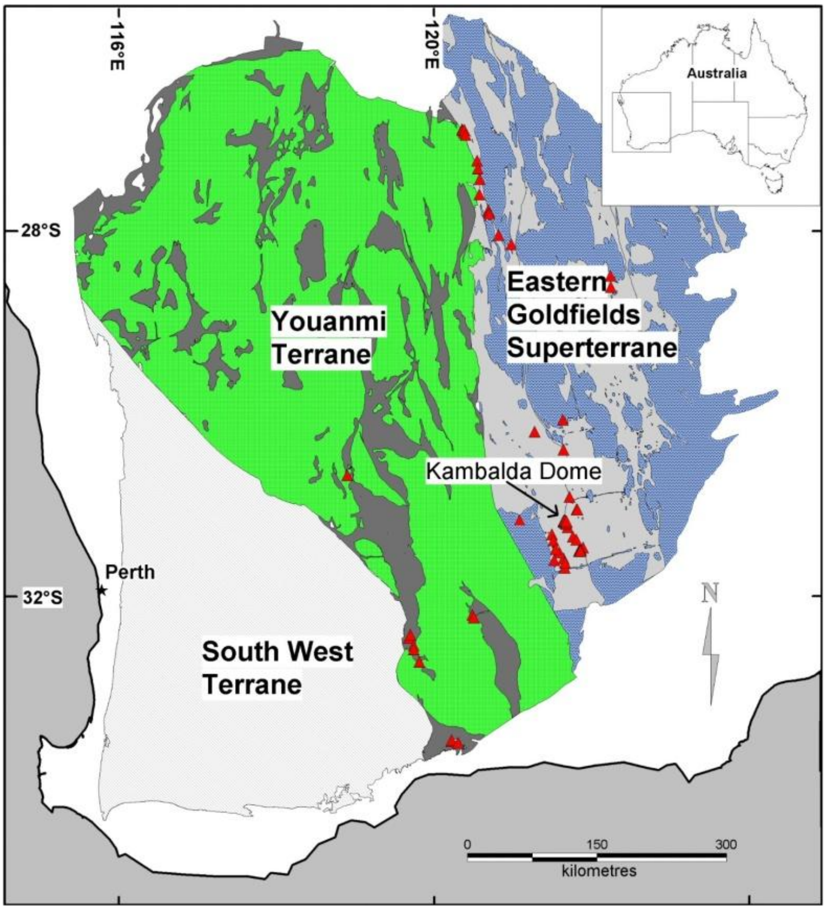

Figure 41. Regional map of the Yilgarn Craton modified from Cassidy et al. (2006). Nickel deposits are shown as red triangles and the Kambalda Dome is outlined.

The Kambalda Sequence is unconformably overlain by the Kalgoorlie Sequence (Black Flag and White Flag Formations), which comprises four unconformably bound sequences, characterised by andesite, dacite, and rhyolite volcaniclastic and epiclastic rocks with minor mafic lavas and sedimentary rocks (Woodall, 1965; Travis et al., 1971; Hunter, 1993; Hand, 1998; Krapež et al., 2000). Age determinations constrain the deposition of the Kalgoorlie Sequence to between 2686 ± 3 Ma and 2658 ± 3 Ma (Krapež et al., 2000). The Kalgoorlie Sequence has been interpreted to represent deposition in a series of deep-marine intra-arc basins within an extensional to transtensional tectonic environment (Hand, 1998; Brown et al., 2001; Krapež and Hand, 2008).

The Kurrawang and Merougil sequences unconformably overlie the Kalgoorlie Sequence (Krapež et al., 2000). The Kurrawang Sequence comprises an upwards-fining succession of conglomerate, sandstone, and mudstone, interpreted to represent high-density, coarse-grained to low-density, fine-grained turbidites (Krapež et al., 2000). The Merougil Sequence also consists of upward-fining successions of conglomerates and sandstones, but is interpreted to represent fluvial bar and channel systems (Krapež et al., 2000).

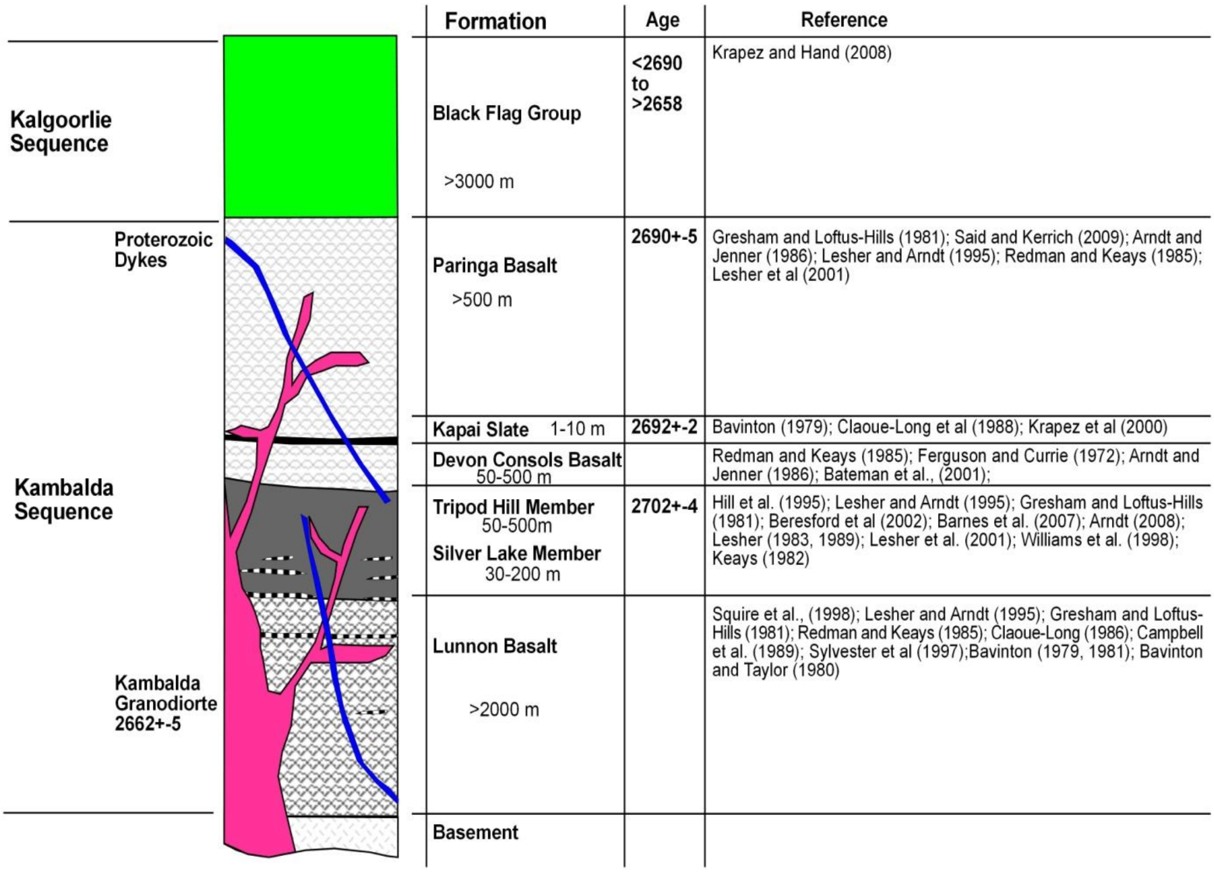

Figure 42. Stratigraphic sequence of the Kambalda and Kalgoorlie Sequences. Modified from Lesher and Arndt (1995) Beresford et al. (2002), Krapež and Hand (2008). Stratigraphy adapted from Gresham and Loftus-Hills (1981), Cowden and Roberts (1990), Swager et al. (1992), Krapež (1997). Ages based on U–Pb SHRIMP data from Claoue-Long et al. (1988), Krapez et al. (2000), Kositcin et al. (2008).

Kambalda Sequence stratigraphy

As the focus of this discussion is primarily concerned with the setting of nickel sulphide mineralisation in the Kambalda Dome, the following detailed stratigraphic summary is limited to those units contained within the Kambalda Sequence and underlying basement, and will not discuss the overlying Kalgoorlie, Kurrawang, and Merougil Sequences.

Basement

Over the years, various studies have speculated on the nature of the basement underlying the Kambalda Dome stratigraphy. A number of lines of indirect evidence support the presence of an older basement. Ages >3.4 Ga are identified within the cores of xenocrystic zircons from samples of the Lunnon Basalt, Devon Consuls, and Paringa Basalts (Compston et al., 1986), with subsequent metamorphic overgrowths occurring between 3.2 to 3.1 Ga, and final overgrowths dated at 2.7 Ga (Compston et al., 1986). Trace element and isotopic data support the hypothesis that magmas from the Kambalda Sequence (i.e. Lunnon Basalt – Kambalda Komatiite – Devon Consols – Paringa Basalt) may have been generated through varying degrees of crustal contamination (Arndt and Jenner, 1986) and mixing of a depleted mantle source with an enriched subcontinental lithospheric mantle (Said and Kerrich, 2009).

Lunnon Basalt

The Lunnon Basalt forms the footwall to the Kambalda Komatiite Formation and is at least 2000 m thick, dominated by thin, 2–30 m flows, with a minimum lateral extent of 500 km^2 (Kambalda to Tramways, extending to Bluebush in the south; Squire et al., 1998). Stratigraphically equivalent basalts are observed throughout the Eastern Goldfields Terrane, and potentially represent 1.5 million km^3 of erupted basalt (Lesher and Arndt, 1995).

Four lithological facies are identified within the Lunnon Basalt and consist of: pillowed basalts, massive basalt, basalt breccia, and sulphidic metasediments (Squire et al., 1998). Pillowed flows contribute c. 45% of Lunnon Basalt stratigraphy and commonly exhibit well defined rims with radial and sub-concentric perlitic fractures, and associated periodic flow-top breccia (Gresham and Loftus-Hills, 1981; Squire et al., 1998). Massive basalts comprise c. 45% of the sequence and are dominated by fine- to medium-grained basalt flows ranging in thickness from 10–140 m. It is thought that the Lunnon Basalt erupted in an aqueous environment with at least 700 m of water depth (Squire et al., 1998), and that eruption was generally passive with magma transport through lava tubes on an average slope of <10° with paleo-flow towards the west, ranging from southwest to north-northwest (Squire et al., 1998).

The Lunnon Basalt tholeiites are characterised by moderately high MgO contents, high Ni and Cr abundances, low incompatible element concentrations, and minor LREE depletion (La/Sm_n = 0.76 to 0.85; Redman and Keays, 1985). The basalts have been subdivided into an upper and lower sequence, separated by interflow sediments. The lower basalts (high-Mg series basalts; HMSB) are slightly less evolved (0.69% TiO_2, 8.3% MgO) and contain olivine phenocrysts, whereas the upper basalts (low-Mg series basalt; LMSB) are more evolved (0.91% TiO_2, 7.8% MgO) and do not contain olivine phenocrysts (Redman and Keays, 1985). Vesicles and amygdales are observed in the lower sequence but absent from the upper sequence (Squire et al., 1998).

The Lunnon Basalts are interpreted to have formed during decompression melting of a mantle plume in the subcontinental lithospheric mantle, which was depleted in LREE by a previous small-degree partial melt extraction (Redman and Keays, 1985; Campbell et al., 1989). Geochemistry and isotope work indicates a possible mixed source for their generation, with a combination of both depleted and primitive mantle sources (Lesher and Arndt, 1995; Said and Kerrich, 2009).

Sediments

Metasedimentary units occur throughout the Kambalda Sequence, but are predominantly intercalated within the Silver Lake Member of the Kambalda Komatiite, rather than within the Lunnon Basalt, where sediments are commonly thin and discontinuous. Rare sedimentary structures (e.g. low-angle cross lamination, small scale scours, and scour truncations) are locally observed and indicate a very-low energy depositional environment, in either deep or quiet shallow conditions (Squire et al., 1998). A thin sedimentary horizon is documented in a number of drill intersections approximately 100–200 m below the contact between the Lunnon Basalt and the overlying Kambalda Komatiite Formation. This horizon represents a rather continuous stratigraphic marker, which divides the geochemically less evolved from the slightly more evolved basalts in the Lunnon Basalt Sequence (Gresham and Loftus-Hills, 1981; Redman and Keays, 1985). Sediment abundance increases towards the top of Lunnon Basalt, with the unconformity between mafic and ultramafic units marked by a thin (≤ 5 m) stratigraphic sedimentary horizon (contact sediments of Bavinton, 1981).

Within the Silver Lake Member of the Kambalda Komatiite Formation, interflow sediments (internal sediments of Bavinton, 1981) are intercalated with komatiite flows, defining the boundary between successive flow lobes. Xenocrystic zircon age determinations of 2702 ± 4 Ma were derived from the sediments (Claoue-Long et al., 1988). In the Silver Lake Member there is a general (with very few exceptions; cf. Bavinton, 1979, 1981) antithetic spatial relationship between the localisation of nickel sulphide mineralisation, which is generally hosted within channelised/trough-like environments, and the sediments, which are dominantly restricted to the flanking environments, and are ubiquitously absent from the ore prism/channel facies and a 100–300 m wide zone flanking the channel (Bavinton, 1981).

Interflow sedimentary units have limited lateral continuity and are only continuous over 200–500 m, with highly variable thickness (Bavinton, 1981). The sediments are interpreted to attain a cumulative maximum thickness at a distance of c. 500 m from the channel facies, thinning towards the channel (Bavinton, 1981). Stratigraphically above the Silver Lake Member, interflow sediments progressively disappear, with only a few thin discontinuous intervals reported in the Tripod Hill Member (Bavinton, 1979; Gresham and Loftus-Hills, 1981).

Three main types of sediments have been documented within the Kambalda Dome area and described in detail by Bavinton (1979, 1981). In decreasing abundance they consist of: 1) light grey to white siliceous cherts, 2) dark grey to black carbon-bearing slates, and 3) dark-green chlorite and amphibolite-rich non-siliceous units. Sediment samples typically contain 20–25 wt% iron sulphide in the form of pyrrhotite in thin 5–15 mm layers, and periodically as small trains of spherical sulphide nodules parallel to the apparent layering. Total sulphide content increases up through the stratigraphy.

Sediment–ore association

Sediments are not commonly found associated with ore zones (Fig. 43). This has led to the interpretation that thermo-mechanical assimilation of sediments occurred within the channel environment, where turbulent magma effectively scoured the sediments upon emplacement of the komatiite units (Lesher, 1983; Lesher et al., 1984). Consequently, the assimilation of sulphur led the komatiites to sulphide saturation. Most ore zones are characterised by a trough-like feature hosting mineralisation, with an abrupt transition to a barren contact, commonly containing a 5–30 cm thick chlorite zone. The basal chlorite zone grades laterally into planar metasediments, which are dominantly cherty in appearance (Bavinton, 1979). Sediment distribution in the Kambalda Dome is best summarised by Gresham and Loftus-Hills (1981), where 'approximately 60–70% of the ultramafic–basalt contact at the Kambalda Dome is sediment-bearing, and the majority of sediment-free contact areas contain ore'.

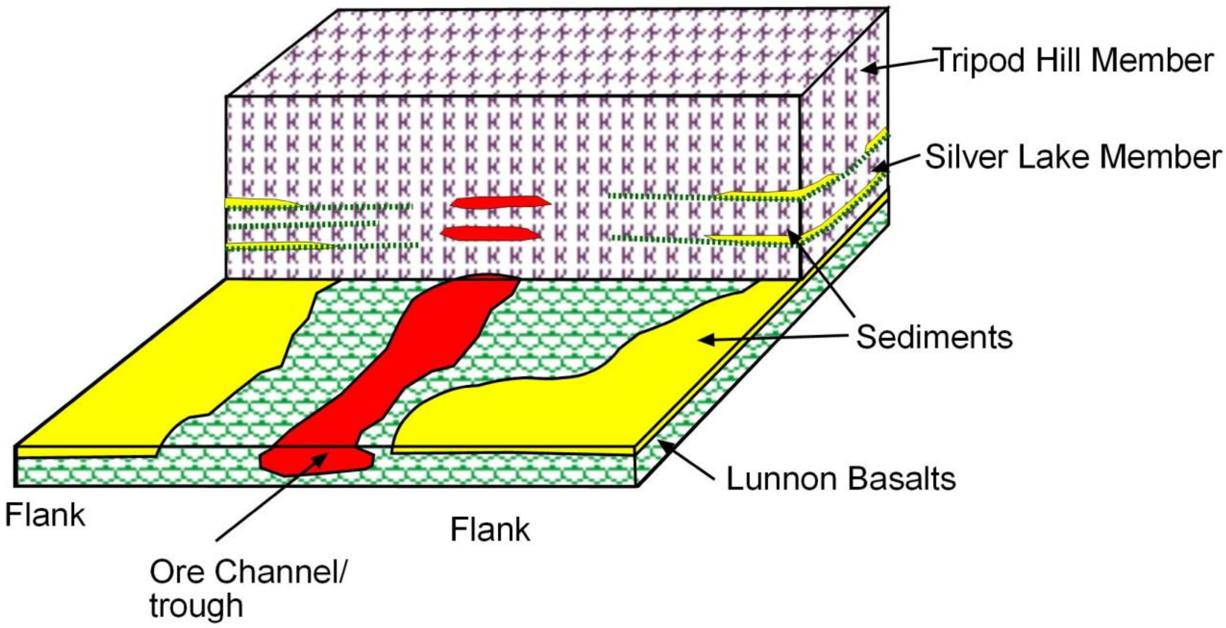

Figure 43. Block model showing distribution of contact sediments within the channel and flank facies. Modified from Gresham and Loftus-Hills (1981), and Stone and Masterman (1998).

Kambalda Komatiite Formation

Stratigraphy and volcanology

Silver Lake Member

The Silver Lake Member comprises approximately one-third of the Kambalda Komatiite Formation and varies in thickness from 50–200 m. The Silver Lake Member consists of one or more laterally continuous flow units, characterised by thick ortho-mesocumulate channels, and thinner flanking environments (Hill et al., 1995; Lesher and Arndt, 1995; Beresford et al., 2002). Nickel sulphide mineralisation is associated with thickened (>30 m) channels, whereas flanking facies environments are commonly barren. The basal flow channel is interpreted to reside in a shallow (5–30 m deep), pre-existing linear topographic feature, which was further modified by thermo-mechanical erosion and/or deformation (Gemuts and Theron, 1975; Lesher et al., 1984;

Groves et al., 1986; Lesher, 1983, 1989; Stone and Archibald, 2004; Stone et al., 2005; Williams et al., 1998).

Channel facies environments attain thicknesses of up to 100 m and are generally characterised by olivine ortho-mesocumulates. Thickened olivine cumulates are the product of sustained lava flow and continuous olivine accumulation with variable abundance of chromite (Hill et al., 1995). Consequently, channel environments are interpreted to be highly dynamic systems, and contain complex cooling histories within B-zone cumulates. B-zone cumulates commonly represent multiple composite cooling units, with the formation of spinifex (<1–10 m thick) at the flow top forming only once flow velocity has decreased, post-dating a portion of the lower B-zone olivine accumulation (Hill et al., 1995; Lesher and Arndt, 1995). We refer to Arndt et al. (2008) and Barnes (2006) for a comprehensive discussion of komatiitic textures and volcanological features.

Flanking environments of the Silver Lake Member commonly have a constant thickness of 15–35 m. Flanks exhibit a well-differentiated sequence of A-zone spinifex and B-zone cumulates dominated by orthocumulates. Thin interflow metasedimentary units are common in the flanking environment, ranging in thickness from <1–10 m. The relationship between channel and flanking facies is addressed in detail by Beresford et al. (2002).

Tripod Hill Member

The Tripod Hill Member comprises approximately the upper two-thirds of the Kambalda Komatiite Formation observed in the Kambalda Dome. The Tripod Hill Member ranges in thickness from 100–1000 m, and is thickest on the northern and western flanks of the Kambalda Dome, and thinner on the eastern flank and in the St Ives, Tramways, and Bluebush areas to the south (Lesher and Arndt, 1995; Beresford et al., 2002). The Tripod Hill Member is characterised by thin (1–10 m) well-differentiated komatiite flow units. Flows exhibit well-developed flow top breccia, thick spinifex zones, and well-developed B-zone cumulates (Gresham and Loftus-Hills, 1981).

Spinifex-textured samples from the Tripod Hill Member range from 15–32 wt% MgO, 0.4 – 0.5 wt% TiO_2, 440–920 ppm Ni, and 2500–4020 ppm Cr (Lesher and Arndt, 1995). Overall, komatiite flows are characterised by a lower MgO content than in the underlying Silver Lake Member, the result of a lower overall proportion of cumulus olivine. Within the Tripod Hill Member, a trend of decreasing MgO content up-sequence is observed (Gresham and Loftus-Hills, 1981). Metasediments are generally absent from the Tripod Hill Member. The Tripod Hill Member displays LREE enrichment relative to the Silver Lake Member, the result of minor (c. 5%) crustal contamination (Lesher and Arndt, 1995). In terms of chalcophile element concentrations, the Tripod Hill Member displays normal background values (i.e. not enriched or depleted; cf. Lesher et al., 2001). Accordingly, it is likely that these komatiites did not equilibrate with any sulphide liquid during crystallisation and fractionation.

Devon Consuls Basalt and Paringa Basalt

Overlying the Kambalda Komatiite Formation is a sequence of mafic volcanic and intrusive bodies. In the Kambalda Dome, the transition from the underlying ultramafic units (Kambalda Komatiite) to the mafic volcanic units is generally sharp, with the exception of St Ives and Tramways, where the mafic and ultramafic units display interfingering relationships (Gresham and Loftus-Hills, 1981). The mafic units are siliceous high magnesium series basalts (SHMSB) comprising two members: the Devon Consuls Basalt (lower member) and the Paringa Basalt (upper member; Redman and Keays, 1985). Both members contain abundant (up to 30%) phenocryst phases of olivine, pyroxene, and feldspar (Redman and Keays, 1985). The Kapai Slate, which is a thin (1–10 m) sedimentary unit, separates the two members.

The Devon Consuls Basalt has a total thickness of 60–100 m and is characterised by two lithologies: 1) pillowed flows with felsic ocelli, and 2) massive komatiitic basalt with minor pillowed phases (Ferguson and Currie, 1972). The basalts are further classified into two geochemical groups: 1) high-Si, low-Mg basalt characterised by 52–60 wt% SiO_2, 4–6 wt% MgO, 6.7 – 7.4 wt% FeO_{tot}, 0.71 – 0.83 wt% TiO_2, 742–896 ppm Cr, 231–278 ppm Ni; and 2) low-Si, high-Mg basalt characterised by 47–52 wt% SiO_2, 9–16 wt% MgO, 9.8 – 12 wt% FeO_{tot}, 0.64 – 0.77 wt% TiO_2, 576–1173 ppm Cr, 152–393 ppm Ni (Redman and Keays, 1985; Arndt and Jenner, 1986). Trace element data of the Devon Consuls Basalt exhibit flat HREE primitive mantle normalised patterns with moderate LREE enrichment and no apparent Nb depletion (Arndt and Jenner, 1986; Bateman et al., 2001). Undepleted chalcophile element abundances within the unit indicate that the basalt lavas were emplaced sulphide undersaturated (Redman and Keays, 1985; Lesher et al., 2001). SHRIMP and U–Pb age determinations of xenocrystic zircon contained within the Devon Consuls Basalt exhibit a range of ages from 3450 ± 3 Ma to 2652 ± 12 Ma (Compston et al., 1986). Two geochrons are identified, where the oldest (3385 ± 10 Ma) represents crystallisation age of the basement, and a younger (2693 ± 50 Ma) is the age of basaltic volcanism (Compston et al., 1986).

The Kapai Slate is subdivided into two facies assemblages: a lower carbonaceous shale and an upper unit, which comprises incised turbidites and carbonaceous shales (Krapež et al., 2000). Lithologically, the Kapai slate is composed of carbonaceous shales, with minor, pale, cherty sediments and felsic volcaniclastic rocks (Bavinton, 1979; Bateman et al., 2001). Xenocrystic zircon age determinations from the Kapai Slate produced minimum ages of 2692 ± 4 Ma, with grains as old as 3441 ± 18 Ma (Claoue-Long et al., 1988).

The Paringa Basalt (upper member) exceeds 500 m in thickness and is dominated by massive or pillowed mafic flows. Massive units are interpreted as either massive sheet flows or intrusive units, and commonly contain medium- to coarse-grained differentiated portions in the central sections (Gresham and Loftus-Hills, 1981; Said and Kerrich, 2009). The Paringa Basalt rocks are characterised by c. 10.6 wt% MgO, 10.7 wt% FeO, 13.0 wt% Al_2O_3 1070–2020 ppm Cr, 280–470 ppm Ni with strong LREE-enrichment (Arndt and Jenner, 1986; Lesher and Arndt, 1995).

The Paringa Basalt is subdivided based on geochemistry into a lower enriched basalt, characterised as komatiitic basalt to high-magnesium tholeiitic basalt (HMTB), and an upper depleted basalt, characterised as HMTB (Said and Kerrich, 2009). The upper depleted basalt exhibits a narrow compositional range (Mg# 61–75) and a flat primitive mantle normalised pattern with slight LREE depletion. The lower enriched basalt is characterised by Mg# from 53–76 with LREE-enriched primitive mantle normalised patterns (Bateman et al., 2001; Said and Kerrich, 2009).

The enriched Paringa Basalt (lower unit), characterised by LREE enrichment with negative anomalies at Nb and Ti, was initially interpreted by Barley (1986) as a crustally contaminated ultramafic unit. However, Said and Kerrich (2009) indicated that the disparity in geochemistry between the two Paringa Basalt geochemical subunits can be attributed to a mantle plume interacting with the asthenospheric mantle that had a component of older crust recycled back into it (Said and Kerrich, 2009). Despite displaying a complex petrogenetic history, the Paringa Basalt lavas were emplaced sulphide-undersaturated and preserve normal chalcophile element concentrations (Redman and Keays, 1985; Lesher et al., 2001).

Intrusions

A complex sequence of intrusions post-dates and crosscuts the mafic and ultramafic units of the Kambalda Sequence stratigraphy. Geochronology indicates that the majority of these granitoid intrusions were emplaced between 2.70 to 2.63 Ga, both coeval with and post-dating felsic volcanism of the Kalgoorlie Sequence (Brown et al., 2001). Intrusion lithologies vary from biotite monzogranites, granodiorites to trondhjemites (Witt and Swager, 1989; Champion and Sheraton, 1993, 1997; Witt and Davy, 1997).

Geochemistry

The Silver Lake Member of the Kambalda Komatiite Formation comprises Munro-type komatiites with initial liquid compositions of up to 30 wt% MgO (Lesher et al., 1984; Lesher, 1989; Lesher and Arndt, 1995). Olivine in equilibrium with the initial liquid would be approximately Fo_{94}, similar to that observed within the channel facies olivine cumulate zones (Ross and Hopkins, 1979; Lesher, 1989). The Silver Lake Member komatiites exhibit major and trace element variations consistent with the fractionation and accumulation of olivine and minor chromite, akin to other Munro-type komatiite systems (Barnes et al., 2004, 2007). Accumulation of pyroxene is not observed in the channel facies. However, pyroxene (metamorphosed to amphibole) is prevalent in the more fractionated flanking facies of the Silver Lake Member and is interpreted to reflect the fractionated composition of magmas in this environment (Lesher and Arndt, 1995).

Channel facies are characterised by >40 wt% MgO and inferred olivine compositions ranging from $Fo_{90–94}$ (Ross and Hopkins, 1979; Lesher, 1989; Barnes et al., 2007). Channel facies spinifex ranges in composition from 16–31% MgO, 0.31 – 0.53 wt% TiO_2, 385–1610 ppm Ni, 1280–3670 ppm Cr; rare earth element abundances are characterised by La/Sm_n ratios from 0.4 – 0.7 with slight LREE depletion over HREE (Lesher and Arndt, 1995). Conversely, flanking facies cumulates are characterised by lower MgO contents (35–40% MgO) and olivine compositions ranging from $Fo_{89–91}$. Spinifex-textured samples from the flanks are commonly characterised by 12–21 wt% MgO, 0.41 – 0.55 wt% TiO_2, 424–1810 ppm Cr, and 71–410 ppm Ni, with LREE enrichment relative to the channel spinifex (Lesher and Arndt, 1995).

Although thermo-mechanical assimilation of crustal material occurred upon komatiite emplacement (Groves et al., 1986; Williams et al., 1998; Bekker et al., 2009), channel environments from the Silver Lake Member do not generally exhibit evidence of crustal contamination, displaying LREE depletion (La/Sm_{cn} of 0.6 – 0.7) and chondritic ratios of MREE and HFSE (Al_2O_3/TiO_2 ~ 20, Ti/Zr = 97, Gd/Yb_{cn} = 1; Arndt and Jenner, 1986). However, evidence of crustal contamination is locally recorded in the flanking facies (Lesher and Arndt, 1995; Lesher et al. 2001), as observed with LREE enrichment. It is argued that geochemical evidence of crustal contamination is only preserved in the flanks and not in the channels because of the highly dynamic nature of komatiite systems. In fact, in the channels the assimilation and contamination process that occurred upon thermo-mechanical erosion of the substrate is generally followed by extensive magma recharge, effectively removing and diluting any geochemical signature of this interaction. Conversely, magma recharge in the flanks is less pronounced and preservation of a crustal contamination signature is permitted (Lesher and Arndt, 1995; Lesher et al., 2001). Throughout the Kambalda Dome komatiite system, there is very little physical evidence of contamination: locally, felsic ocelli, which may be derived from sediment assimilation, are identified along channel margins (Frost, 1985; McNaughton et al., 1988; Frost and Groves, 1989; Frost, 1992).

For a comprehensive review of PGE geochemistry of the Silver Lake Member of the Kambalda Komatiite Formation, we refer to Heggie (2010) and Fiorentini et al. (in press). The authors integrated a large body of high-precision PGE analyses from various locations, with a focus on the Long–Victor system on the eastern flank of the Kambalda Dome, and investigated the complex relationship between PGE variation and localisation of different styles of nickel sulphide mineralisation (Fig. 44). The authors concluded that the Silver Lake Member komatiites generally display background PGE concentrations typical of other 2.7 Ga Munro-type komatiites globally (Maier et al., 2009). Anomalously PGE depleted samples are rare and generally concentrated on the flanking environments of large channelised environments. Conversely, samples from the channels are either undepleted or display anomalous PGE enrichment.

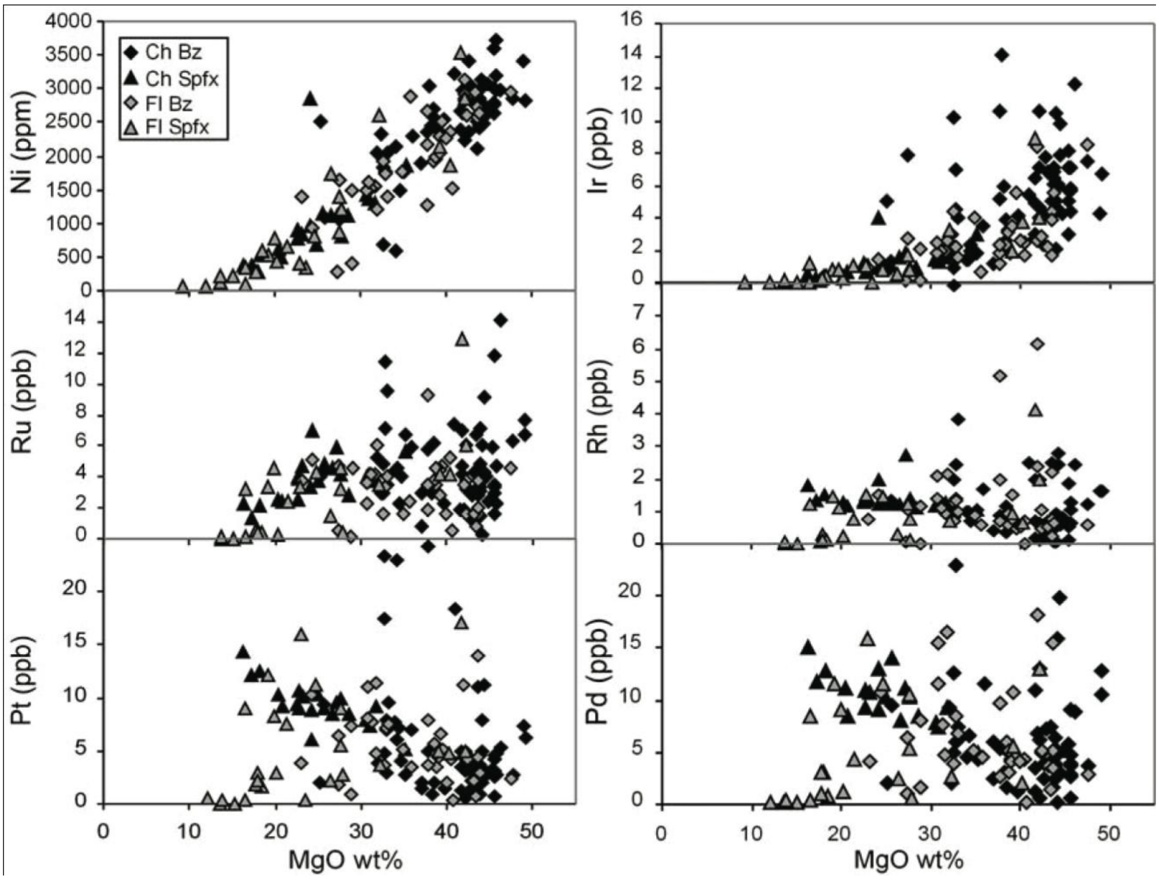

Figure 44. Relationship between MgO content and chalcophile element concentrations from samples collected at the Long–Victor deposit, located on the eastern flank of the Kambalda Dome (cf. Figure 45). All data are labelled according to volcanic facies where samples where collected: Ch Bz = B zone from channelised environments; Ch Spfx = A zone from channelised environments; Fl Bz = B zone from flanking environments; Fl Spfx = A zone from flanking environments. Data from Heggie (2010).

Nickel sulphide mineralisation

Mineralisation setting

Basal contact mineralisation occurs at the contact between the footwall basalts and the overlying ultramafic flows. Basal contact ore surfaces occur within embayments or depressions in the top of the footwall basalts, termed troughs or channels (Lesher, 1983). The formation of trough or embayment features is still contentious with two existing interpretations. The first interpretation states that thermal-mechanical erosion of flowing ultramafic lavas was responsible for the down-cutting and entrenchment of the ultramafic flows into the sediments overlying the pillowed basalts (Lesher, 1983, 1989; Beresford et al., 2005). The second interpretation suggests a strong structural control on the troughs, either through pre-existing faults with syn-eruption graben development, or during subsequent deformation of the greenstone belt (Stone and Archibald, 2004; Stone et al., 2005). Evidence for both interpretations is extensively documented, and a combination of both (pre-existing structures/topography and the erosive action of the ultramafic magma followed by regional deformation) is most likely responsible for the current ore surface configuration.

Troughs within the Kambalda Dome area vary in size, but are commonly narrow and elongate with lengths up to 2300 m and widths <300 m (Gresham and Loftus-Hills, 1981). Mineralisation within major troughs is dominantly continuous, yet occurs as small (20–130 m) elliptical ore bodies in minor troughs.

Hangingwall ore occurs stratigraphically higher but usually within 100 m of the komatiite–basalt contact (Gresham and Loftus-Hills, 1981). Hangingwall mineralisation within the Lunnon, Hunt, and McMahon ore shoots (Fig. 45) occurs at the contact of the basal ultramafic flow unit and the second flow unit, with nickel sulphides residing on the A-zone spinifex of the basal flow (Groves et al., 1986).

Finally, structurally mobilised ore is characterised by the mechanical transportation of sulphide into areas of dilation and lower tectonic pressure (e.g. fold hinges, fault dilation zones, shear zones) away from the primary accumulation site (Lesher and Keays, 2002). Mobilised ore is restricted to massive sulphides, because they are generally more ductile than disseminated sulphide (cf. McQueen, 1981, 1987).

Mineralisation style

Basal and strata-bound mineralisation zones are commonly 1–3 m thick, with intervals up to 10 m thick. Mineralisation consists of a massive sulphide layer, (<1m thick) overlain by a zone of matrix mineralisation. Massive sulphide ore is defined as >80% sulphide comprising pyrrhotite, pentlandite, pyrite, and chalcopyrite with minor spinels concentrated at some basal or top contacts (Groves et al., 1977). Massive ore is generally banded with alternating layers of pyrrhotite- and pentlandite-rich bands. These bands formed during recrystallisation under directed stress, and are generally parallel to the adjacent wallrock contacts (Ewers and Hudson, 1972).

Matrix mineralisation is defined as mineralisation with 40–80% sulphide abundance, with the remainder comprising serpentine or talc, pseudomorphs after original olivine, within a continuous matrix of sulphide. In the Kambalda Dome area, matrix mineralisation exhibits a gradation of sulphide abundance from 40–60% at the top, to 60–80% sulphide at the base of the unit, and ranges in thickness from 1–3 m (Gresham and Loftus-Hills, 1981; Keays et al., 1981). Matrix mineralisation exhibits a greater lateral continuity than the massive sulphide.

Finally, disseminated mineralisation is rarely observed within the Kambalda Dome area. However, disseminated mineralisation is observed in both basal contact and strata-bound settings. Disseminated mineralisation is characterised by <10–40%, commonly 5% interstitial sulphide within an ultramafic host.

Orthomagmatic mineralisation in the Kambalda Dome

The eastern flank of the Kambalda Dome contains the Gibb, Long, and Victor ore shoots. These ore shoots are characterised by dominant basal contact mineralisation with strong structural control on trough development or modification (for a review on the genesis and development of throughlike embayments see Beresford et al., 2002; Stone and Archibald, 2004). Sediments are generally absent from within the ore environment of the shoots. However, contact sediments are observed in the flanking positions to the troughs, and hanging-wall sediments are observed in the flanks, and can stratigraphically overlap the trough structures.

The Gibb ore shoot (Fig. 45), up-dip of the Long ore shoot, is 1300 m in length and attains a maximum width of 150 m. The Gibb shoot is arc-like, plunging shallowly to the north and south and terminated at the northern end by extensive felsic intrusions. Ni-sulphide mineralisation is hosted within the basal komatiite flow, which attains a maximum thickness of 50 m. The mineralisation resides in a complex trough structure dominated by basalt-basalt pinch-outs (Gresham and Loftus-Hills, 1981).

The Long ore shoot (Fig. 45) occurs down dip of the Gibb ore shoot and has a known plunge length of 2300 m, and remains open both up- and down-plunge (giving rise to the Long North and Long South targets of Independence Group and recent discoveries of the Moran and McLeay ore bodies; Fig. 45). The Long shoot attains a maximum width of 300 m and is characterised by steep to sub-vertical dips, but appears to shallow as it plunges to the south. Mineralisation is contained within a low-relief trough structure, within the basal komatiite flow which attains a thickness of c. 100 m.

The Victor ore shoot (Fig. 45), south of the Gibb shoot, represents its down-plunge extension, separated by extensive felsic intrusions. The basal flow unit attains thicknesses of >75 m within the trough, has a defined mineralised plunge length of 850 m, and another 700 m of unmineralised extension prior to the development of the McLeay ore body. Nickel sulphide mineralisation within the Victor shoot occurs in a well-defined trough structure c. 200 m in width, and is defined by high-angle normal faulting up dip and low angle reverse faulting down dip.

Alteration and metamorphism

Alteration and metamorphism studies on the Kambalda Dome have been conducted by Ross (1974), Barrett et al. (1977), Bavinton (1979), Marston and Kay (1980), Gresham and Loftus-Hills (1981), Arndt and Jenner (1986), Barley and Groves (1987), and summarised by Swager and Griffin (1990) and Lesher et al. (2001). Komatiite units in the Kambalda Dome have undergone seafloor hydrothermal alteration with alteration intensity (i.e. serpentinisation) increasing towards the top of the succession (Barley and Groves, 1987). Later regional metamorphism comprising further serpentine alteration and talc–carbonate alteration locally overprints the primary seafloor alteration assemblage.

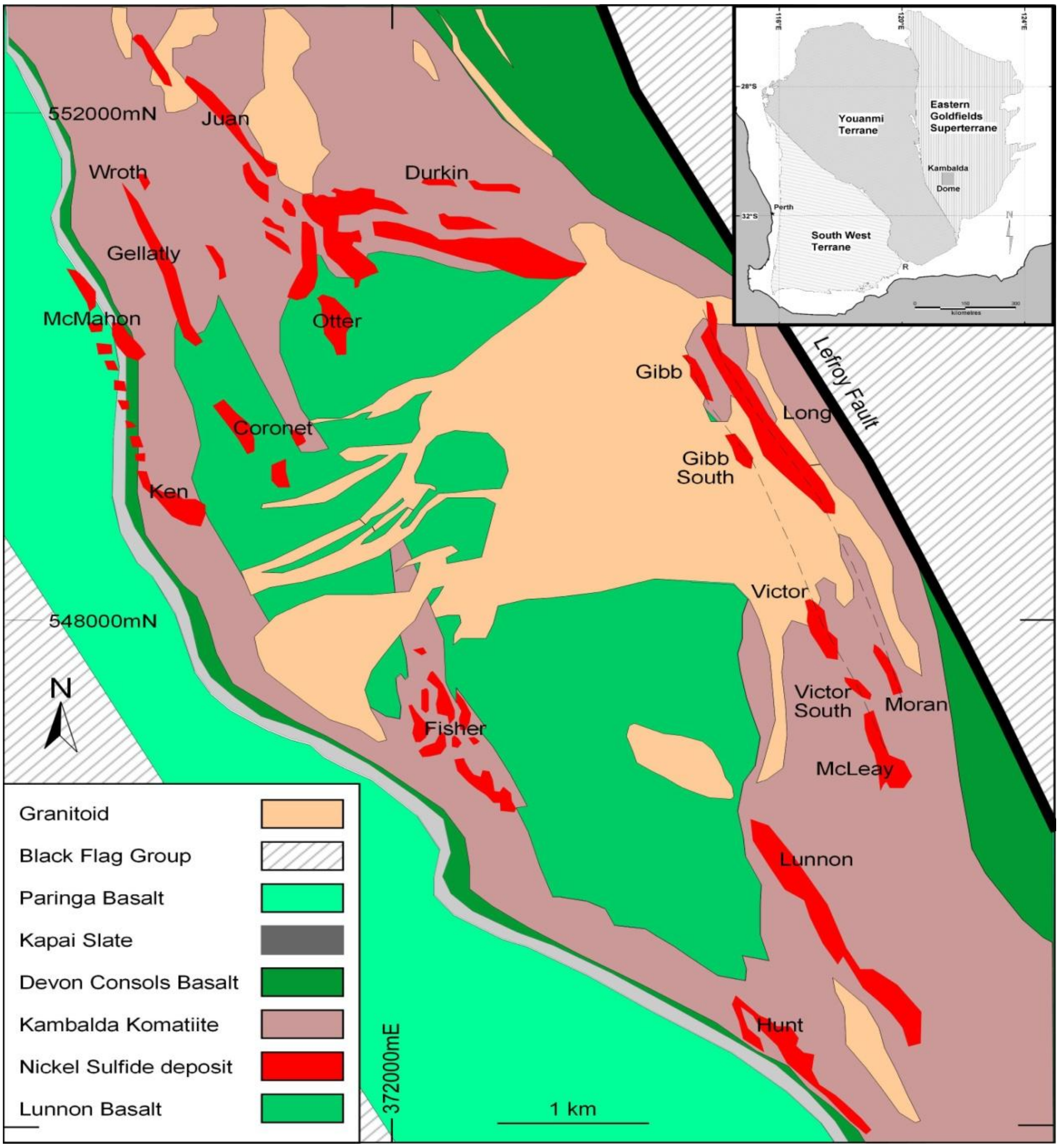

Figure 45. Geological map of the Kambalda Dome area with mineralised nickel sulphide ore shoots projected to surface. Major ore shoots are labelled. Map projection UTM zone 16 with WGS84 datum.

Regional metamorphism in the Kalgoorlie Terrane (e.g. Kambalda Dome) is dominantly upper greenschist facies, but exhibits variation from prehnite–pumpellyite to lower amphibolite facies. Metamorphism occurred at low to intermediate pressure (2.5 ± 1 kb to >4.5 kb) and temperatures of 500–600°C, with peak metamorphism occurring during late D2 to D3 (Binns et al., 1976; Bavinton, 1979; McQueen, 1981; Bickel and Archibald, 1984; Wong, 1986). Low-grade metamorphism is associated with the central cores of the greenstone belts, whereas higher grades are observed along the periphery (Brown et al., 2001).

Texturally, many primary igneous features are still visible within the lithological units around the Kambalda Dome, yet complete replacement by alteration assemblages has occurred locally. The limited development of penetrative deformation fabrics also aids in the preservation of primary igneous textures. Progressive mineralogical changes through hydrothermal alteration were observed in the ultramafic lithologies (Gresham and Loftus-Hills, 1981; Cowden and Roberts, 1990). Glass and pyroxene were progressively hydrated to form tremolite and chlorite, whereas olivine is altered to serpentine. Antigorite was identified as the dominant serpentine mineral and either formed via direct serpentinisation of olivine at peak metamorphic conditions, or is a result of prograde metamorphism of a lizardite assemblage. Progressive carbonation of the serpentinites resulted in destruction of tremolite and antigorite and the formation of talc–dolomite and talc–magnesite assemblages. The only relict igneous minerals are chromite and rare portions of cumulate olivine within the Durkin and Victor shoots of the Kambalda Dome (Gresham and Loftus-Hills, 1981; Lesher, 1983).

Alteration effects on sulphide mineralisation are variable and highly dependent upon the metals involved, abundance of sulphide, and alteration conditions. Work on the Mt Keith disseminated ore body shows the progressive upgrading and Ni-enrichment of the sulphides with alteration (Donaldson, 1981; Grguric et al., 2006). However, recent work by Barnes et al. (2010) indicates that high tenor nickel sulphide assemblages may be primary and not require secondary enrichment. Furthermore, progressive alteration at the Black Swan deposit and selected ore shoots in the Kambalda Dome has shown limited effects on the composition of mineralisation (Lesher and Campbell, 1993; Barnes, 2004; Barnes et al., 2009).

Komatiite lithologies are especially susceptible to element redistribution due to the reactive nature of high-MgO rocks during low-grade metamorphism. Overall, most komatiite systems exhibit high loss on ignition values (during XRF whole rock analysis) attributed to the addition of volatiles to the system. More advanced alteration and metamorphism has variable effects on the geochemistry and mobility of elements within these systems (Arndt and Jenner, 1986; Lahaye et al., 1995; Lesher and Arndt, 1995; Kerrich and Wyman, 1996; Lesher and Stone, 1996). Large ion lithophile elements (LILE; Cs, Rb, K, Na, Ba, Sr, Ca, Eu^{+2}), with large ionic radii and low charge, have high susceptibility for mobilisation during alteration events (Xie et al., 1993; Lesher and Arndt, 1995; Lahaye et al., 1995). The mobility of LILE varies from local remobilization, complete removal or enrichment within the system during seafloor alteration, hydrothermal alteration, and regional metamorphism.

Rare earth element and high field strength element mobility is dependent upon fluid composition, with CO_2-rich fluids having a stronger influence on element mobility than H_2O-rich fluids (Lahaye et al., 1995). Light rare earth elements (LREE: La, Ce, P, Nd) are relatively immobile, yet may become mobile in CO_2-rich fluids. Limited mobility is observed at low fluid/rock ratios for the high field strength elements (U^{+4}, Th, Ta, Nb, Zr, Y, and HREE), aluminium, the first period transition elements (Sc, Ti, V, Cr; Mn, Co, Ni) and the highly siderophile elements (Fe and PGE).

Sulphur mobility within nickel sulphide systems of the Kambalda Dome was proposed by Marston and Kay (1980), Seccombe et al. (1981) and McQueen (1987). However, work by Keays et al. (1981) on ore tenors and chalcophile elements in the silicate host rocks did not show a strong relationship between sulphur and the metal abundance in samples containing <0.2 wt% sulphur. The lack of correlation between the two was attributed to metamorphic and metasomatic redistribution of only S (± Au and Cu). Work by Seccombe et al. (1981) and Stone et al. (2004) identified sulphur loss through oxidation from prograde metamorphism, with disseminated sulphides being more susceptible to sulphur loss than net-textured and massive sulphides. Lesher and Campbell (1993) identified post crystallisation mobilisation of sulphur with no systematic correlation between degree of sulphur mobility and change in chalcophile element abundance.

Alteration effects on PGE abundances in whole-rock samples are perhaps the most difficult to identify, leading to the inference of limited PGE mobility during alteration. However, PGE-enriched hydrothermal ore deposits have been identified (Hanley, 2006; Wilde, 2005), and PGE mobility and fractionation during weathering is documented (Cameron and Hattori, 2005; Traoré et al., 2008) in aqueous solutions at very high salinities and oxidation states (Wood and Norman, 2008), thus supporting PGE mobility in sulphur poor rocks under certain conditions. However, PGE immobility is documented at the Black Swan deposit, which is characterised by pervasive talc–carbonate alteration (Barnes et al., 2004).

Geodynamic setting of the Kambalda Nickel Camp

The Kambalda Nickel Camp represents one of the largest komatiite-associated nickel sulphide systems in the world (Barnes, 2006). Refining our understanding of the ore forming process at the deposit scale may provide useful information in order to constrain the geometry and localisation of specific ore zones, but it does not provide insights into why the Kambalda Nickel Camp is where it is. Conversely, it is crucial to constrain the geodynamic environment that permitted the formation of such an endowed domain and the clustering of so many mineralised systems in a restricted area.

According to the mineral systems approach defined by McCuaig et al. (2010), in order to fully comprehend the salient features that control the clustering of mineralised systems it is necessary to investigate a wide range of data sets at multiple scales. Accordingly, it is necessary to also identify the lithospheric controls on the localisation of the Kambalda Nickel Camp. Figure 46a illustrates the Nd model age map of the Yilgarn Craton of Western Australia (Champion and Cassidy, 2007), whereas Figure 46b is a simplified geological map, which outlines the setting of the largest nickel sulphide systems. Figures 47a and b show a close up of the Kambalda domain of the Kalgoorlie Terrane.

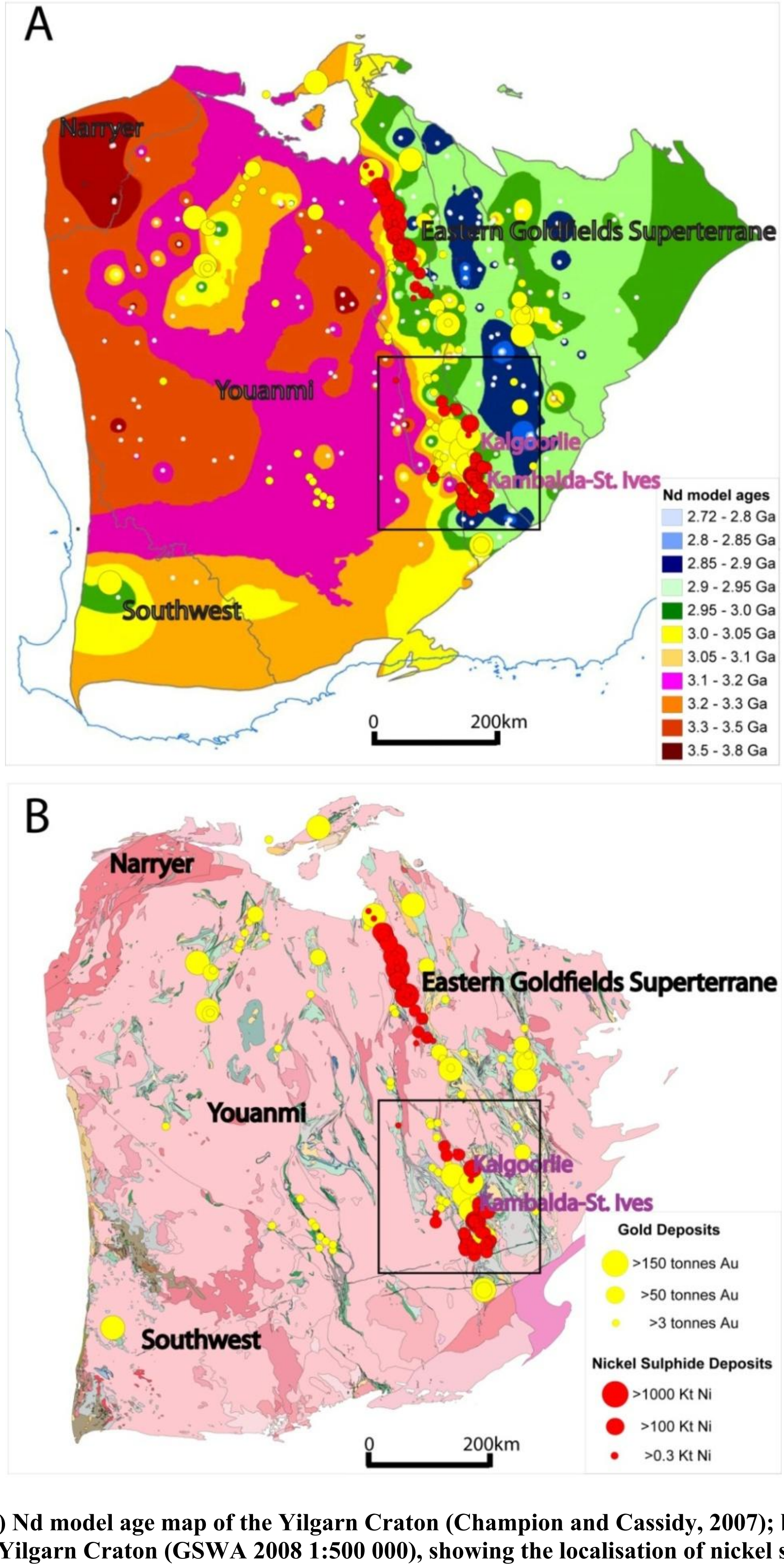

Figure 46 a) Nd model age map of the Yilgarn Craton (Champion and Cassidy, 2007); b) geological map of the Yilgarn Craton (GSWA 2008 1:500 000), showing the localisation of nickel sulphide deposits in the Eastern Goldfields Superterrane. Inset area outlined by square is shown in Figure 47. From McCuaig et al. (2010). See Chapter 1, Figure 19 for data sources.

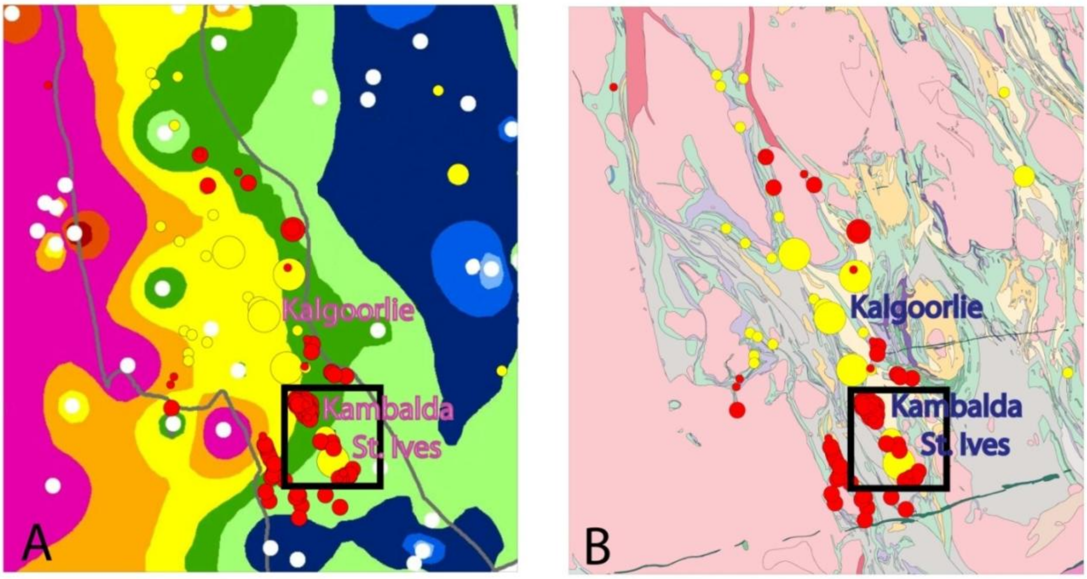

Figure 47. Inset from Figure 46: a) Nd model age map of the Kambalda domain in the Kalgoorlie Terrane (Champion and Cassidy, 2007); b) geological map of the Kambalda domain in the Kalgoorlie Terrane (GSWA 2008, 1:500 000), showing the localisation of nickel sulphide and gold deposits. The black box highlights the Kambalda Nickel Camp locations. From McCuaig et al. (2010).

The isotopic map is interpreted as providing a snapshot of the lithosphere architecture at c. 2.65 Ga. This map can be utilised as a proxy to image the major lithospheric discontinuities, which may have acted as active pathways for large volumes of hot mantle-derived melt to reach upper crustal levels without undergoing any significant differentiation. In other words, steep colour gradients (interpreted as lithosphere scale boundaries) in the isotopic map in Figure 46a show areas of where hot magmas were most likely emplaced.

All along the Kalgoorlie Terrane, from Wiluna in the north to south of the Kambalda Dome, highly mineralised komatiites (e.g. Mount Keith, Perseverance, Black Swan, Kambalda) are localised along the boundary between the isotopically juvenile Eastern Goldfields Superterrane and the older Youanmi Terrane. Arguably, this boundary may represent a significant lithospheric discontinuity at c. 2.7 Ga, along which high volumes of hot komatiites could be emplaced and interact with crustally derived sulphur (cf. Bekker et al., 2009) to generate giant nickel sulphide ore systems. Figure 47 shows how the spatial relationship between nickel sulphide mineralisation and the lithospheric boundary, as reflected by the different isotopic nature of the Youanmi and Eastern Goldfields Superterrane, holds down to the camp scale (Mole et al., 2009; Champion and Cassidy, 2007). On Figure 47 it is noted that the greenstone belts strike NNW, yet the camps of nickel sulphide mineralisation appear to follow the arc of the paleocraton margin imaged by the Nd model age map.

References

Arndt, NT and Jenner, GA 1986, Crustally contaminated komatiites and basalts from Kambalda, Western Australia: Chemical Geology, v. 56, p. 229–255

Arndt, NT, Lesher, CM and Barnes, SJ 2008, Komatiite: Cambridge University Press, Cambridge, UK, 467p.

Barley ME and Groves, DI 1987, Hydrothermal alteration of Archaean supracrustal sequences in the central Norseman–Wiluna belt, Western Australia, *in* Recent advances in understanding Precambrian Gold deposits *edited by* SE Ho and DI Groves: University of Western Australia, Geology Department and University Extension, Publication 11, p. 51–66.

Barnes, SJ, Fiorentini, ML, Godel, BM, Locmelis, M and Ryan, CG 2010, Origin of nickel-rich sulphide assemblages in the Betheno deposit, Yakabindie, WA: evidence from synchrotron X-ray fluorescence mapping *in* Earth Systems: change, sustainability, vulnerability: Geological Society of Australia, 20th Australian Earth Science Convention, Abstracts; Canberra, Australian Capital Territory, 4–8 July 2010, p.113–114

Barnes, SJ 2004, Komatiites and nickel sulfide ores of the Black Swan area, Yilgarn Block, Western Australia. 4: Platinum group element distribution in the ores, and genetic implications: Mineralium Deposita, v. 39, p. 752–765.

Barnes, SJ 2006, Komatiite-hosted nickel sulfide deposits: geology, geochemistry, and genesis, *in* Nickel Deposits of the Yilgarn Craton: Geology, Geochemistry, and Geophysics applied to Exploration *edited by* SJ Barnes: Society of Economic Geologists, Special Publication No. 13, p. 50–97.

Barnes, SJ, Gole, MJ and Hill, RET 1988, The Agnew nickel deposit, Western Australia: Part II: sulfide geochemistry, with emphasis on the platinum group elements: Economic Geology, v. 83, p. 537–550.

Barnes, SJ, Hill, RET and Evans, NJ 2004a, Komatiites and nickel sulfide ores of the Black Swan area, Yilgarn Craton, Western Australia. 3: komatiite geochemistry, and implications for ore forming processes: Mineralium Deposita, v. 39, p. 729–751.

Barnes, SJ, Hill, RET, Perring, CS and Dowling, SE 2004b, Lithogeochemical exploration for komatiite-associated Ni-sulfide deposits: strategies and limitations: Mineralogy and Petrology, v. 82, p. 259–293.

Barnes, SJ, Lesher, CM and Sproule, RA 2007, Geochemistry of komatiites in the Eastern Goldfields Superterrane, Western Australia and the Abitibi Greenstone Belt, Canada, and implications for the distribution of associated Ni–Cu–PGE deposits: Applied Earth Science, v. 116, p. 167–187.

Barnes, SJ, Wells, MA and Verrall, MR 2009, Effects of magmatic processes, serpentinization, and talc–carbonate alteration on sulfide mineralogy and ore textures in the Black Swan disseminated nickel sulfide deposit, Yilgarn Craton: Economic Geology, v. 104, p. 539–562.

Barrett, FM, Binns, RA, Groves, DI, Marston, RJ and McQueen, KG 1977, Structural history and metamorphic modification of Archean volcanic-type nickel deposits, Yilgarn Block, Western Australia: Economic Geology, v. 72, p. 1195–1223.

Batemann, R, Costa, S, Swe, T and Lambert, D 2001, Archaean mafic magmatism in the Kalgoorlie area of the Yilgarn Craton, Western Australia: a geochemical and Nd isotopic study of the petrogenetic and tectonic evolution of a greenstone belt: Precambrian Research. v. 108, p. 75–112.

Bavinton, OA 1979, Interflow sedimentary rocks from the Kambalda ultramafic sequence: Australia National University, Canberra, Australian Capital Territory, PhD thesis (unpublished).

Bavinton, OA 1981, The nature of sulfidic metasediments at Kambalda and their broad relationships with associated ultramafic rocks and nickel ore: Economic Geology, v. 78, p. 1606–1628.

Bavinton, OA and Keays, RR 1978, Precious metal values from interflow sedimentary rocks from the komatiite sequences at Kambalda, Western Australia: Geochimica et Cosmochimica Acta, v. 42, p. 1151–1163.

Bavinton, OA and Taylor, SR 1980, Rare earth element geochemistry of Archean metasedimentary rocks from Kambalda, Western Australia: Geochimica et Cosmochimica Acta, v. 44, p. 639–648.

Bekker, A, Barley, ME, Fiorentini, ML, Rouxel, OJ, Rumble, D and Beresford, SW 2009, Atmospheric sulfur in Archean komatiite-hosted nickel deposits: Science, v. 326, p. 1086–1089.

Beresford, S, Cas, R, Lahaye, Y and Jane, M 2002, Facies architecture of an Archean komatiite-hosted Ni-sulfide ore deposit, Victor, Kambalda, Western Australia: implications for komatiite lava emplacement: Journal of Volcanology and Geothermal Research, v. 118, p. 57–75.

Beresford, S, Stone, WE, Cas, R, Lahaye, Y and Jane, M 2005, Volcanological controls on the localization of the komatiite-hosted Ni–Cu–(PGE) Coronet Deposit, Kambalda, Western Australia: Economic Geology, v. 100, p. 1457–1467.

Bickel, MJ and Archibald, NJ 1984, Chloritoid and staurolite stability — implications for metamorphism in the Archaean Yilgarn Block in Western Australia: Journal of Metamorphic Petrology, v. 2, p. 179–203.

Binns, RA, Gunthorpe, RJ and Groves, DI 1976, Metamorphic patterns and development of greenstone belts in the eastern Yilgarn Block, *in* The Early History of the Earth *edited by* BF Windley: John Wiley and Sons, London, UK, p. 303–316.

Brown, SJA, Krapež, B, Beresford, SW, Cassidy, KF, Champion, DC, Barley, ME and Cas, RAF 2001, Archean volcanic and sedientary environments of the Eastern Goldfields Province Western Australia – a field guide: Geological Survey of Western Australia, Record 2001/13, 66p.

Campbell, IH and Hill, RI 1988, A two-stage model for the formation of the granite–greenstone terrains of the Kalgoorlie-Norseman area, Western Australia: Earth and Planetary Science Letters, v. 90, p. 11–25.

Campbell, IH, Griffiths, RW and Hill, RI 1989, Melting in an Archean mantle plume: heads it's basalts, tails it's komatiites: Nature, v. 339, p. 697–699.

Cameron, EM and Hattori, KH 2005, Platinum group elements in geochemical exploration, *in* Exploration for Platinum Group Element Deposits *edited by* JE Mungall: Mineralogical Association of Canada, Short Course, Volume 35, p. 287–303.

Cassidy, KF, Champion, DC, Krapež, B, Barley, ME, Brown, SJA, Blewett, RS, Groenewald, PB and Tyler, IM 2006, A revised geological framework for the Yilgarn Craton, Western Australia: Geological Survey of Western Australia, Record 2006/8, 8p.

Champion, DC and Sheraton, JW 1993, Geochemistry of granitoids in the Leonora–Laverton region, Eastern Goldfields Province, *in* Kalgoorlie '93. An International Conference on Crustal Evolution, Metallogeny and Exploration of the Eastern Goldfields, Extended Abstracts *edited by*PR Williams: Geoscience Australia, Record 1993/54, p. 39–54.

Champion, DC and Sheraton, JW 1997, Geochemistry and Nd isotope systematics of Archaean granites in the Eastern Goldfields, Yilgarn Craton, Australia: implications for crustal growth models: Precambrian Research, v. 83, p. 109–132.

Champion, DC and Smithies, RH 2004, Archean Granites, *in* The Ishihara Symposium: Granites and Associated Metallogenesis *edited by* P Blevin, M Jones, and B Chappell: Geoscience Australia, record 2003/14, p. 13–19.

Champion, DC, Cassidy, KF and Smithies, RH 2006, Sm–Nd isotope characteristics of the Pilbara and Yilgarn Cratons, Western Australia: Implications for crustal growth in the Archean *in* Geochemistry downunder: 16th Goldschmidt Conference, Melbourne, Victoria, 27 August – 1 September 2006, Abstracts; Geochimica et Cosmochimica Acta, v. 70, Suppl. 1, p. A95.

Champion, DC and Cassidy, KF 2007, An overview of the Yilgarn Craton and its crustal evolution *in* Proceedings of Geoconferences (WA) Inc. Kalgoorlie '07 Conference, Kalgoorlie, Western Australia *edited by* FP Bierlein and CM Knox-Robinson: Geoscience Australia Record, 2007/14, p. 8–12.

Chauvel, C, Dupré, B and Jenner, GA 1985, The Sm–Nd age of Kambalda volcanics is 500 Ma too old!: Earth and Planetary Science Letters, v. 74, p. 315–324.

Claoué-Long, JC, Thirlwall, MF and Nesbitt, RW 1984, Revised Sm–Nd systematics of Kambalda greenstones, Western Australia: Nature, v. 307, p. 697–701.

Claoué-Long, JC, Compston, W and Cowden, A 1988, The age of the Kambalda greenstones resolved by ion-microprobe: implications for Archean dating methods: Earth and Planetary Science Letters, v. 89, p. 239–259.

Compston, W, Williams, IS, Campbell, IH and Gresham, JJ 1986, Zircon xenocrysts from the Kambalda volcanics: age constraints and direct evidence for older continental crust below the Kambalda–Norseman greenstones: Earth and Planetary Science Letters, v. 76, p. 299–311.

Cowden, AC 1988, Emplacement of komatiite lava flows and associated nickel sulfides at Kambalda, Western Australia: Economic Geology, v. 83, p. 436–442.

Cowden, A and Archibald, NJ 1987, Massive-sulfide fabrics at Kambalda and their relevance to inferred stability of monosulfide solid-solution: Canadian Mineralogist, v. 25, p. 37–50.

Cowden, A and Roberts, DE 1990, Komatiite hosted nickel sulphide deposits, Kambalda, *in* Geology of Mineral Deposits of Australia and Papua New Guinea *edited by* FE Hughes: Australasian Institute of Mining and Metallurgy, Melbourne, Victoria, p. 567–581.

Doepel, JJG 1973, Norseman, Western Australia: Geological Survey of Western Australia,1:250 000 Geological Series Explanatory Notes, 40p.

Donaldson, MJ 1981, Redistribution of ore elements during serpentinization and talc–carbonate alteration of some Archean dunites, Western Australia: Economic Geology, v. 76, p. 1698–1713.

Ewers, WE and Hudson, DR 1972, An interpretative study of nickel-iron sulfide ore intersections. Lunnon Shoot, Kambalda, Western Australia: Economic Geology, v. 67, p. 1075–1092.

Ferguson, J and Currie, KL 1972, Silicate immiscibility in the ancient ‘basalts’ of the Barberton Mountain Land, Transvaal: Nature Physical Science, v. 235, p. 86–89.

Fiorentini, ML, Barley, ME, Pickard, A, Beresford, SW, Rosengren, NM, Cas, RAF and Duuring, P 2005, Age constraints of the structural and stratigraphic architecture of the Agnew–Wiluna greenstone belt: implications for the age of komatiite–felsic association and interaction in the Eastern Goldfields Province, Western Australia: MERIWA, Report 255, Project M356.

Fiorentini, ML, Barnes, SJ, Lesher, CM, Heggie, G, Keays, RR and Burnham, OM in press, Platinum-group element geochemistry of mineralized and non-mineralized komatiites and basalts: Economic Geology.

Foster, JG, Lambert, DD, Frick, LR and Maas, R 1996, Re–Os isotopic evidence for genesis of Archaean nickel ores from uncontaminated komatiites: Nature, v. 382, p. 703.

Frost, KM 1985, Ocellar komatiites at Kambalda, Western Australia: evidence of silicate liquid immiscibility and sediment assimilation: The University of Western Australia, Perth, Western Australia, BSc (Hons) thesis, 121p. (unpublished).

Frost, KM 1992, The role of ground melting in the genesis of komatiite-associated nickel sulfide deposits at Kambalda and Widgiemooltha, Western Australia: The University of Western Australia, Perth, Western Australia, PhD thesis, 239p. (unpublished).

Frost, KM and Groves, DI 1989, Ocellar units in the Kamabalda–Widgiemooltha komatiite sequence: evidence for sediment assimilation by komatiite lavas, *in* Magmatic Sulphides — The Zimbabwe Volume *edited by* MD Prendergast and MJ Jones: Institution of Mining and Metallurgy, London, UK p. 207–214.

Gemuts, I and Theron, A 1975, The Archean between Coolgardie and Norseman — stratigraphy and mineralization, *in* Economic Geology of Australia and Papua New Guinea, v.1, Metals *edited by* CL Knight: The Australasian Institute of Mining and Metallurgy, Parkville, Victoria, Monograph 5, p. 66–74.

Gresham, JJ and Loftus-Hill, GD 1981, The Geology of the Kambalda Nickel Field, Western Australia: Economic Geology, v. 76, p. 1373–1416.

Grguric, BA, Rosengren, NM, Fletcher, CM and Hronsky, JMA 2006, Type 2 Deposits: Geology, mineralogy, and processing of the Mount Keith and Yakabindie orebodies, Western Australia, *in* Nickel Deposits of the Yilgarn Craton: Geology, Geochemistry, and Geophysics applied to exploration *edited by* SJ Barnes: Society of Economic Geologists, Special Publication No. 13, p. 119–138.

Groves, DI, Barrett, FM, Binns, RA and McQueen, KG 1977, Spinel phases associated with metamorphosed volcanic-type iron-nickel sulfide ores from Western Australia: Economic Geology, v. 72, p. 1224–1244.

Groves, DI, Korkiakoski, EA, McNaughton, NJ, Lesher, CM and Cowden, A 1986, Thermal erosion by komatiites at Kambalda, Western Australia and the genesis of nickel ores: Nature, v. 319, p. 136–139.

Hand, JL 1998, The sedimentological and stratigraphic evolution of the Archaean Black Flag Beds, Kalgoorlie, Western Australia: implications for regional stratigraphy and basin setting of the Kalgoorlie Terrane: Monash University, Melbourne, Victoria, PhD thesis (unpublished).

Hall, HIE and Bekker, C 1965, Gold deposits of Norseman, *in* Geology of Australian Ore Deposits *edited by* J McAndrew: Australasian Institute of Mining and Metallurgy; 8th Commonwealth Mining and Metallurgical Congress, Melbourne, Victoria, p.101–107.

Hanley, JJ 2006, The aqueous geochemistry of the platinum-group elements (PGE) in surficial, low-T hydrothermal and high T-magmatic-hydrothermal environments, *in* Exploration for Platinum Group

Element Deposits *edited by* JE Mungall: Mineralogical Association of Canada, Short Course Volume 35, p. 35–50.

Heggie, G 2010, The spatial variation of PGE in barren and mineralised komatiite systems: The University of Western Australia, Perth, Western australia, PhD thesis (unpublished).

Hill, RI, Campbell, IH and Compston, W 1989, Age and origin of granitic rocks in the Kalgoorlie–Norseman region of Western Australia: Implications for the origin of Archaean crust: Geochimica et Cosmochimica Acta, v. 53, p. 1259–1275.

Hill, RI, Chappell, BW and Campbell, IH 1992, Late Archaean granites of the southeastern Yilgarn Block, Western Australia: age, geochemistry, and origin: Transactions of the Royal Society of Edinburgh, Earth Sciences, v. 83, p. 211–226.

Hill, RET, Barnes, SJ, Gole, MJ and Dowling, SE 1995, The volcanology of komatiites as deduced from field relationships in the Norseman–Wiluna greenstone belt, Western Australia: Lithos, v. 34, p. 159–188.

Hunter, WM 1993, Geology of the granite–greenstone terrane of the Kalgoorlie and Yilmia 1:100 000 sheets, Western Australia: Geological Survey of Western Australia, Report 35, 91p.

Keays, RR 1982, Palladium and iridium in komatiites and associated rocks: application to petrogentic problems, *in* Komatiites *edited by* NT Arndt and EG Nisbet: Allen and Unwin, London, UK, p. 435–457.

Keays, RR, Ross, JR and Woolrich, P 1981, Precious metals in volcanic peridotite-associated nickel sulfide deposits in Western Australia. II: Distribution within the ores and host rocks at Kambalda: Economic Geology, v. 76, p. 1645–1674.

Kerrich, R and Wyman, DA 1996, The trace element systematics of igneous rocks in mineral exploration: an overview *in* Trace Element Geochemistry of Volcanic Rocks: Applications for Massive Sulphide Exploration *edited by* DA Wyman: Geological Association of Canada, Short Course Notes, v. 12, p. 1–50.

Kositcin, N, Brown, AJA, Barley, ME, Krapez, B, Cassidy, KF and Champion, DC 2008, SHRIMP U–Pb zircon age constraints on the Late Archaean tectonostratigraphic architecture of the Eastern Goldfields Superterrane, Yilgarn Craton, Western Australia: Precambrian Research, v. 161, p. 5–33.

Krapež, B 1997, Sequence-stratigraphic concepts applied to the identification of depositional basins and global tectonic cycles: Australian Journal of Earth Sciences, v. 44, p. 1–36.

Krapež, B and Hand, JL 2008, Late Archaean deep-marine volcaniclastic sedimentation in an arc-related basin: the Kalgoorlie Sequence of the Eastern Goldfields Superterrane, Yilgarn Craton, Western Australia: Precambrian Research, v. 161, p. 89–113.

Krapež, B, Brown, SJA, Hand, J, Barley, ME and Cas, RAF 2000, Age constraints on recycled crustal and supracrustal sources of Archean metasedimentary sequences, Eastern Goldfields Province, Western Australia: evidence from SHRIMP zircon dating: Tectonophysics, v. 322, p. 89–133.

Lahaye, Y, Arndt, NT, Byerly, G, Chauvel, C, Fourcade, S and Gruau, G 1995, The influence of alteration on the trace-element and Nd isotopic compositions of komatiites: Chemical Geology, v. 126, p. 43–64.

Lesher, CM 1983, Localization and genesis of komatiite-associated Fe–Ni–Cu sulphide mineralization at Kambalda, Western Australia: The University of Western Australia, Perth, Western Australia, PhD thesis, 199p. (unpublished).

Lesher, CM 1989, Komatiite associated nickel sulfide deposits *in* Ore deposits associated with magmas: Reviews in Economic Geology, v. 4, p. 45–101.

Lesher, CM and Arndt, NT 1995, REE and Nd isotopic geochemistry, petrogenesis and volcanic evolution of contaminated komatiites at Kambalda, Western Australia: Lithos, v. 34, p. 127–157.

Lesher, CM and Campbell, IH 1993, Geochemical and fluid dynamic modeling of compositional variations in Archean Komatiite-hosted nickel sulfide ores in Western Australia: Economic Geology, v. 88, p. 804–816.

Lesher, CM and Stone, WE 1996, Exploration geochemistry of komatiites, *in* Igneous Trace Element Geochemistry Applications for Massive Sulphide Exploration *edited by* DA Wyman: Geological Association of Canada, Short Course Notes, v. 12, p. 153–204.

Lesher, CM and Keays, RR 2002, Komatiite-associated Ni–Cu–PGE deposits: geology, mineralogy, geochemistry, and genesis *in* The Geology, Geochemistry, Mineralogy, and Mineral Beneficiation of Platinum-Group Elements *edited by* LJ Cabri: Canadian Institute of Mining, Metallurgy and Petroleum, Special Volume 54, p. 579–618.

Lesher, CM, Arndt, NT and Groves, DI 1984, Genesis of komatiite-associated nickel sulphide deposits at Kambalda, West-Australia: A distal volcanic model, *in* Sulphide deposits in mafic and ultramafic rocks *edited by* DL Buchan and ML Jones: Institution of Mining and Metallurgy;Proceedings of International Geological Correlation Program, Projects 161 and 91, Third Nickel Sulphide Field Conference, Perth, Western Australia, p. 70–80.

Lesher, CM, Burnham, OM, Keays, RR, Barnes, SJ and Hulbert, L 2001, Trace-element geochemistry and petrogenesis of barren and ore-associated komatiites: Canadian Mineralogist, v. 39, p. 673–696.

Maier, WD, Barnes, SJ, Campbell, IH, Fiorentini, ML, Peltonen, P, Barnes, S-J and Smithies, H 2009, Mantle magmas reveal progressive mixing of meteoric veneer into the early Earth's deep mantle: Nature, v. 460, p. 620–623.

Marshall, B and Gilligan, LB 1987, An introduction to remobilization: information from ore-body geometry and experimental considerations: Ore Geology Reviews, v. 2, p. 87–131.

Marshall, B and Gilligan, LB 1993, Remobilization, syn-tectonic processes and massive sulphide deposits: Ore Geology Reviews, v. 8, p. 39–64.

Marshall, B, Vokes, FM and Larocque, ACL 2000, Regional metamorphic remobilization: upgrading and formation of ore deposits, *in* Metamorphosed and Metamorphogenic Ore Deposits *edited by* PG Spry, B Marshall and FM Vokes: Reviews in Economic Geology, v. 16, p. 19–38.

Martin, H 1994, The Archaean grey gneisses and genesis of continental crust, *in* Crustal Evolution *edited by* KC Condie: Elsevier, Amsterdam, The Netherlands, p. 205–259.

Marston, RJ and Kay, BD 1980, The distribution, petrology, and genesis of nickel ores at the Juan Complex, Kambalda, Western Australia: Economic Geology, v. 75, p. 546–565.

Marston, RJ, Groves, DI, Hudson, DR and Ross, JR 1981, Nickel sulfide deposits in Western Australia: a review: Economic Geology, v. 76, p. 1330–1363.

Mason, R, Hodkiewicz, P, Barrett, D and Buerger, R 2003, Structural geology of the Emily Ann nickel deposit and implications for the mining process: Australasian Institute of Mining and Metallurgy; 5th International Mining Geology Conference, Bengido, Voctoria, 17–19 November 2003, p. 155–170.

McCuaig, TC, Beresford, SW and Hronsky, J 2010, Translating the mineral systems approach into an effective exploration targeting system: Ore Geology Reviews, v. 38, p. 121–127 <doi:10.1016/j.oregeorev.2010.05.008>

McNaughton, NJ, Frost, KM and Groves, DI 1988, Ground melting and ocellar komatiites: a lead isotopic study at Kambalda, Western Australia: Geological Magazine, v. 125, p. 285–295.

McQueen, KG 1981, Volcanic-associated nickel deposits from around the Widgiemooltha Dome, Western Australia: Economic Geology, v. 76, p. 1417–1443.

McQueen, KG 1987, Deformation and remobilization in some Western Australian nickel ores: Ore Geology Reviews, v. 2, p. 269–286.

Mole, D, Fiorentini, ML, Thébaud, N, McCuaig, TC and Cassidy, K 2009, Using LA-ICP-MS Lu–Hf SHRIMP dating to investigate tectonostratigraphic controls on the localisation of Archaean komatiite-hosted nickel-sulphide deposits and camps in the Yilgarn craton, Western Australia: The Mineralogical

Society; Micro-analysis, Processes, Time (MAPT) Conference, Edinburgh, UK, 31 August –2 September 2009, Programme and abstracts, p. 143–144

Myers, JS 1997, Geology of granite: Journal of the Royal Society of Western Australia, v. 80, p. 87–100.

Nelson, DR 1995, Compilation of SHRIMP U–Pb zircon geochronology data, 1995: Geological Survey of Western Australia, Record 1996/5, 251p.

Nelson, DR 1997, Evolution of the Archaean granite–greenstone terranes of the Eastern Goldfields, Western Australia: SHRIMP zircon constraints: Precambrian Research, v. 83, p. 57–81.

Nelson, DR 1998, Compilation of SHRIMP U–Pb zircon geochronology data, 1997: Geological Survey of Western Australia, Record 1998/2, 196p.

Oversby, VM 1975, Lead isotope systematics and ages of Archean acid intrusives in the Kalgoorlie-Norseman area, Western Australia: Geochimica et Cosmochimica Acta, v. 39, p. 1107–1125.

Plimer, IR 1987, Remobilization in high-grade metamorphic environments: Ore Geology Reviews, v. 2, p. 231–245.

Redman, BA and Keays, RR 1985, Archean basic volcanism in the Eastern Goldfields Province, Yilgarn Block, Western Australia: Precambrian Research, v. 30, p. 113–152.

Ross, JRH 1974, Archaean nickel sulphide mineralization: Lunnon Shoot, Kambalda, Western Australia: University of California, Berkeley, PhD thesis, 283p. (unpublished).

Ross, JR and Hopkins, GMF 1979, Kambalda nickel sulfide deposits, *in* Economic Geology of Australia and Papua New Guinea I. Metals *edited by* CL Kight: Australasian Institute Mining and Metallurgy, Parkville, Victoria, p. 100–121.

Said, N and Kerrich, R 2009, Geochemistry of coexisting depleted and enriched Paringa Basalts, in the 2.7 Ga Kalgoorlie Terrane, Yilgarn Craton, Western Australia: Evidence for a heterogeneous mantle plume event: Precambrian Research, v. 174, p. 289–309.

Seat, Z, Stone, WE, Mapleson, DB and Daddow, BC 2004, Tenor variation within komatiite-associated nickel sulphide deposits: insights from the Wannaway Deposit, Widgiemooltha Dome, Western Australia: Mineralogy and Petrology, v. 82, p. 317–339.

Seccombe, PK, Groves, DI, Marston, RJ and Barrett, FM 1981, Sulfide paragenesis and sulfur mobility in Fe–Ni–Cu sulfide ores at Lunnon and Juan Main Shoots, Kambalda: textural and sulfur isotopic evidence: Economic Geology, v. 76, p. 1675–1685.

Squire, RJ, Cas, RAF, Clout, JMF and Behets, R 1998, Volcanology of the Archaean Lunnon Basalt and its relevance to nickel sulfide-bearing trough structures at Kambalda, Western Australia: Australian Journal of Earth Sciences, v. 45, p. 695–715.

Stone, WE and Archibald, NJ 2004, Structural controls on nickel sulfide ore shoots in Archean komatiite, Kambalda, WA: the volcanic trough controversy revisited: Journal of Structural Geology, v. 26, p. 1173–1194.

Stone, WE and Masterman, EE 1998, Kambalda nickel deposits, *in* Geology of Australian and Papua New Guinea Mineral Deposits *edited by* DA Berkman and DH Mackenzie: Australasian Institute of Mining and Metallurgy, Melbourne, Victoria, p. 347–356.

Stone, WE, Crocket, JH, Fleet, ME and Larson, MS 1996, PGE mineralization in Archean volcanic systems: geochemical evidence from thick, differentiated mafic–ultramafic flows, Abitibi greenstone belt, Ontario, and implications for exploration: Journal of Geochemical Exploration, v. 56, p. 237–263.

Stone, WE, Heydari, M and Seat, Z 2004, Nickel tenor variations between Archaean komatiite-associated nickel sulphide deposits, Kambalda ore field, Western Australia: the metamorphic modification model revisited: Mineralogy and Petrology, v. 82, p. 295–316.

Stone, WE, Beresford, SW and Archibald, NJ 2005, Structural setting and shape analysis of nickel sulfide shoots at the Kambalda Dome, Western Australia: implications for deformation and remobilization: Economic Geology v. 100, p. 1441–1455.

Swager, C 1989, Structure of Kalgoorlie Greenstones — Regional deformation history and implications for the structural setting of the Golden Mile gold deposits: Geological Survey of Western Australia, Report 25, p. 59–84.

Swager, CP and Griffin, TJ 1990, An early thrust duplex in the Kalgoorlie–Kambalda greenstone belt, Eastern Goldfields Province, Western Australia: Precambrian Research, v. 48, p. 63–73.

Swager, CP, Goleby, BR, Drummond, BJ, Rattenbury, MS and Williams, PR 1997, Crustal structure of granite–greenstone terranes in the Eastern Goldfields, Yilgarn Craton, as revealed by seismic reflection profiling: Precambrian Research, v. 83, p. 43–56.

Swager, CP, Witt, WK, Griffin, TJ, Ahmat, AL, Hunter, WM, McGoldrick, PJ and Wyche, S 1992, Late Archaean granite–greenstones of the Kalgoorlie Terrane, Yilgarn Craton, Western Australia, *in* JE Glover and SE Ho: Geology Deptartment (Key Centre) and University Extension, The University of Western Australia, Perth, Western Australia, p. 107–122.

Sylvester, PJ, Campbell, IH and Bowyer, DA 1997, Niobium/uranium evidence for early formation of the continental crust: Science, v. 275, p. 521–523.

Traore, D, Beauvais, A, Chabaux, F, Peiffert, C, Parisot, J-C, Ambrosi, J-P and Colin, F 2008, Chemical and physical transfers in an ultramafic rock weathering profile: Part 1. Supergene dissolution of Pt-bearing chromite: American Mineralogist, v. 93, p. 22–30.

Travis, GA, Woodhall, R and Bartram, GD 1971, The geology of the Kalgoorlie gold field: Geological Society of Australia, Special Publications, v. 3, p. 175–190.

Trofimovs, J, Davis, BK and Cas, RAF 2004, Contemporaneous ultramafic and felsic intrusive and extrusive magmatism in the Archaean Boorara Domain, Eastern Goldfields Superterrane, Western Australia, and its implications: Precambrian Research, v. 131, p. 283–304.

Weinberg, RF, Moresi, L and van der Borgh, P 2003, Timing of deformation in the Norseman–Wiluna Belt, Yilgarn Craton, Western Australia: Precambrian Research, v. 120, p. 219–239.

Wilde, A 2005, Descriptive ore deposit models: hydrothermal and supergene Pt and Pd deposits, *in* Exploration for platinum group element deposits *edited by* JE Mungall: Mineralogical Association of Canada Short Course 35, p. 145–162.

Williams, PR and Whitaker, AJ 1993, Gneiss domes and extensional deformation in the highly mineralised Archaean Eastern Goldfields Province, Western Australia: Ore Geology Reviews, v. 8, p. 141–162.

Williams, DA, Kerr, RC and Lesher, CM 1998, Emplacement and erosion by Archean komatiite lava flows at Kambalda: revisited: Journal of Geophysical Research, v. 103, p. 27533–27549.

Witt, WK 1994, Geology of the Melita 1:100 000 sheet: Geological Survey of Western Australia, Geological Series Explanatory Notes, 63 p.

Witt, WK and Davy, R 1997, Geology and geochemistry of Archaean granites in the Kalgoorlie region of the Eastern Goldfields, Western Australia: a syn-collisional tectonic setting?: Precambrian Research, v. 83, p. 133–183.

Witt, WK and Swager, CP 1989, Structural setting and geochemistry of Archaean I-type granites in the Bardoc-Coolgardie area of the Norseman–Wiluna Belt, Western Australia: Precambrian Research, v. 44, p. 323–351.

Wong, T 1986, Metamorphic patterns in the Kambalda area and their significance to Archaean greenstone belts of the Kambalda-Widgiemooltha area: The University of Western Australia, Perth, Western Australia, BSc (Hons) thesis (unpublished).

Wood, SA and Norman, C 2008, Mobility of palladium chloride complexes in mafic rocks: insight from a flow-through experiment at 25C using air-saturated, acidic and Cl-rich solutions: Mineralogy and Petrology, v. 92, p. 81–97.

Woodall, R 1965, Structure of the Kalgoorlie goldfield: 8th Commonwealth Mining and Metallurgy Congress, Melbourne, v. 1, p. 71–79.

Woodall, R and Travis, GA 1970, The Kambalda nickel deposits, Western Australia: 9th Commonwealth Mining Metallurgy Congress, London, 1969, Proceedings, v. 2, p. 517–533.

Xie, Q, Kerrich, R and Fan, J 1993, HFSE/REE fractionations recorded in three komatiite–basalt sequences, Archean Abitibi greenstone belt: implications for multiple plume sources and depths: Geochimica et Cosmochimica Acta, v. 57, p. 4111–4118.